N71-37102

NASA TECHNICAL TRANSLATION

NASA TT F-13,994

STUDIES OF THE DIFFRACTION OF LIGHT WITH ULTRASONIC WAVES

2. COMMUNICATION. DIFFRACTION OF LIGHT WITH ULTRASONIC WAVES FOR OBLIQUE INCIDENCE OF THE LIGHT ON THE SOUND WAVE FRONT. BRAGG RELFECTION.

Otohiko Nomoto

Translation of: "Studien Uber die Beugung von Licht an Ultraschallwellen. 2. Mitteilung. Beugung von Licht an Ultraschallen bei schiefem Einfall des Lichtes auf die Schallwellenfront. Braggsche Reflexion." Proceedings of the Phys. Math. Soc. of Japan, Vol. 24, 1942, pp. 618-639.

CASE FILE COPY

NATIONAL AERONAUTICS AND SPACE ADMINISTRATION
WASHINGTON, D.C. 20546 OCTOBER 1971

STUDIES OF THE DIFFRACTION OF LIGHT WITH ULTRASONIC WAVES

2. COMMUNICATION. DIFFRACTION OF LIGHT WITH ULTRASONIC WAVES FOR OBLIQUE INCIDENCE OF THE LIGHT ON THE SOUND WAVE FRONT. BRAGG REFLECTION.

Otohiko Nomoto*

ABSTRACT. Light diffraction experiments with advancing ultrasonic waves were performed at 3.22 and 4.71 MHz in transformer oil. Sonic field depths were 600 mm. Diffraction spectra were recorded versus incidenceangles. Orders up to the 21st were observed. Comparison with existing theories is made.

Summary: Several experiments on the diffraction of light with advancing /613** ultrasonic waves have been carried out for oblique incidence of the light on the sound wave front. Ultrasonic frequencies of 3.22 and 4.71 MHz were used in a liquid (transformer oil) having an ultrasonic velocity of about 1500 m/sec. The sonic field depths (lengths of the light paths in the acoustic field) were 60 mm. The diffraction spectra were recorded at various angles of incidence and the intensity distributions of the diffracted light were measured using a photographic-photometric method for the various orders. The intensity of the diffraction spectra was obtained as a function of the incidence angle in this way. The diffraction spectra showed very pronounced intensity maxima at the Bragg incident angles $\varphi_{B_n} = -n\frac{\lambda}{\Lambda}$, $(n=0, \pm1, \pm2, \pm3, \cdots)$, where n is the diffraction

---

*Read on April 2, 1941.

**Numbers in the margin indicate the pagination in the original foreign text.

order, λ is the light wavelength and Λ is the acoustic wavelength. Bragg reflection has not yet been observed in liquids at an ultrasonic frequency below 10 MHz (or, what is the same thing, 3 MHz in gases). Bragg reflections of second and higher orders have not been known up to the present time. Up to the present, the Bragg reflection has only been observed for the first two orders and this in the frequency region above 10 MHz. On the other hand, the observed Bragg reflection is very pronounced here and always extends to the highest observed order of diffraction, such as for example, the 21st order in an experiment with the ultrasonic frequency of 3.22 MHz. This means that at least in the frequency region between 3 to 5 MHz, this Bragg reflection can be considered as the most important characteristic for the intensity distribution of the diffraction spectra produced during the diffraction with ultrasonic waves for oblique incidence. In addition to this sharp Bragg maximum, there are two large but not sharp side maxima at the angles of incidence $\varphi_n=\varphi_{B_n}\pm\frac{\Lambda}{L}$ where φ_{B_n} is the Bragg angle of n^{th} order ($|n|\geq 3$) and L is the acoustic field depth. The side maxima are more complicated and more numerous for the 0^{th} and 1^{st} orders.

The maximum in the total number of diffraction spectra does not occur for /614 normal incidence. Instead there are two principal maxima for both sides of vertical incidence. This means that normal incidence corresponds to the minimum of the diffraction phenomena and not to the maximum. This agrees with my earlier results. This is also true for the dependence of the total intensity of the diffracted light on the angle. Normal incidence does not correspond to the maximum, but to the minimum of the total intensity of the diffracted light.

Unfortunately, none of the theories developed up to the present can be compared with this result. This is because no theory has completely treated the problem of light diffraction with ultrasonic waves for oblique incidence and for ultrasonic intensity which is not too weak, because of the mathematical difficulties. If the results of the David theory, which calculated the Bragg reflections of the first and the second diffraction orders, or the results

of the Rytov theory, which calculated the Bragg reflection of the first order, are extrapolated to higher diffraction orders, then our results can easily be explained on the basis of these theories. The angles of incidence for the principal maximum and the side maxima of the light intensity in the diffraction spectra can immediately be obtained by extrapolation of these theories. A more complete theory is necessary to explain the light intensity itself.

§ 1. Introduction and Theoretical Discussion

Our knowledge of the phenomena of light diffraction with ultrasonic waves is especially incomplete in the case of oblique incidence of light on the acoustic wave front. Systematical investigations of (1) conditions at very high ultrasonic frequencies of 10 MHz and above, where the so-called Bragg reflection occurs, and (2) conditions for relatively low frequencies of 1.5 MHz and below, where the Raman-Nath elementary theory holds, were made and reported in the first communication of this work [1].

For medium ultrasonic frequencies there have been no systematic theoretical or experimental results. There are only fragmentary results which we can summarize by the following three points:

a) Asymmetry of the diffraction spectra.

If the incident direction of the light with respect to the sound direction is only slightly different from normal incidence, then the diffraction spectra to both sides will have zero order, i.e., the spectra of the incoming light /615 will have this property, and will differ in number and intensity. The number of diffraction spectra becomes larger on the same side for which Bragg reflection occurs for even higher ultrasonic frequencies. This asymmetry is so easy to observe that it is difficult to obtain completely symmetrical diffraction spectra. This asymmetry was already noted by Debye and Sears [2], the discoverers of light diffraction with ultrasonic waves, when they carried out their first experiments. Afterwards, this asymmetry was experimentally

investigated by Bar [3], Parthasarathy [4], by this author and by Neumann [6]. The first report [1] already pointed out that such asymmetry does not completely vanish at the lower frequencies of 1 MHz, where the Raman-Nath theory is valid.

Theoretically this asymmetry has been dealt with in no less than ten theories, even though none of the theories has resulted in more than a qualitative statement regarding the possibility of asymmetry for oblique incidence.

b) Central minimum of diffraction phenomena as a function of angles.

The maximum of the total number of diffraction spectra does not occur for normal incidence. Instead there are two principal maxima to both sides of normal incidence. Normal incidence does not correspond to the maximum but to a minimum of the diffraction phenomena. This was first discovered by this author [5]. The same also holds for the angular dependence of the total intensity of the diffracted light (except for zero order), as was verified by Neumann [6]. According to Neumann, this central minimum occurs when the acoustic field depth (length of the light path in the acoustic field) L is large. On the other hand, if this quantity is small, then normal incidence will correspond to the maximum of the diffraction phenomena.

This central minimum also occurs at high ultrasonic frequencies, where Bragg reflection occurs. The cases observed by this author [5] and by Becker [7] are remarkable. In this case, it was only possible to observe the +1 and -1 diffraction orders for their Bragg incident angles using very large ultrasonic frequencies of 30 or 17 MHz. For normal incidence it was not /616 possible to observe any diffraction spectrum.

c) Vanishing of the diffraction phenomena at very large incidence angles.

As the incidence angle increases, the diffraction phenomena become less pronounced even though there are several fluctuations. At very large incidence angles they disappeared completely. All the results obtained up to the present agree on these points.

In the present communication we will describe the results of several systematic experiments which were carried out at medium ultrasonic frequencies (3.22 and 4.71 HMz) and for oblique incidence.

Since the results of these experiments resulted in a somewhat unexpected, very simple and regular Bragg reflection, we will now make some further remarks regarding the Bragg reflection. The highest observed diffraction order was an experiment carried out at 3.22 MHz and resulted in the observation of the 21st order.

The Bragg reflection in the diffraction of light with ultrasonic waves was theoretically treated by Rykov [8], David [9] and Extermann [10]. It was observed experimentally by Rykov. Parthasarathy [11] and by this author [5]. Korff [12] carried out a quantitative investigation. However, both the theoretical and experimental investigations were limited to the case where the ultrasonic intensity is very small, so that only the weak first orders of diffraction (theoretically also the second) appear. In the experiment, we should add that the ultrasonic frequencies are always larger than 10 MHz in liquids (or 3MHz in air).

According to the theory of David, the intensity of the diffraction spectra of order ± 1 in the diffraction with weak ultrasonic waves is as follows:

$$I_{\pm 1}=\left(\frac{\pi \delta n L}{\lambda}\right)^2 \frac{\sin^2 \pi \frac{L}{\Lambda}\left(\varphi' \pm \frac{\lambda'}{2\Lambda}\right)}{\left\{\pi \frac{L}{\Lambda}\left(\varphi' \pm \frac{\lambda'}{2\Lambda}\right)\right\}^2}. \qquad (1)$$

Here Λ is the acoustic wavelength, λ the light wavelength in the acoustic medium, δn the amplitude of the fluctuations in the index of refraction, caused by the ultrasonic waves, L the acoustic field depth and ϕ' the incidence angle in the acoustic medium. The principal maxima in intensity are observed at the Bragg incidence angles

/617

$$\varphi'_{B\pm1}=\mp\frac{\lambda'}{2\Lambda}. \tag{2}$$

In addition, there are also the side maxima at the incidence angles:

$$\varphi_{\nu}'=\varphi_B'\pm\left(p+\frac{1}{2}\right)\frac{\Lambda}{L},\quad (p=1,2,3,\cdots). \tag{3}$$

The following relationship holds between the intensity of the side maximum I_P^N and the intensity of the Bragg maximum I_B:

$$I_{\pm p}^{N}=\frac{\sin^2\left(p+\frac{1}{2}\right)\pi}{\left\{\left(p+\frac{1}{2}\right)\pi\right\}^2}I_B,\quad (p=1,2,3,\cdots). \tag{4}$$

The angles of zero intensity are given by the following expressions and lie between the Bragg maximum and the side maxima and between two adjacent side maxima:

$$\varphi_{\nu}'=\varphi_B'\pm p\frac{\Lambda}{L},\quad (p=1,2,3,\cdots). \tag{5}$$

If ϕ_B is the incidence angle observed in air, then the following relationship can be formed with ϕ_B':

$$\varphi_{B_n}=n_0\varphi'_{B_n}=-\frac{\theta_n}{2}=-\frac{n\lambda}{\Lambda},\quad (n=\pm1,\pm2,\cdots). \tag{6}$$

Here n_0 is the index of refraction of the medium, n is the diffraction order. θ_n is the diffraction angle of n^{th}-order in air and λ the light wavelength in air.

According to the rigorous theory of Extermann, Bragg reflection can only be expected in the case where the acoustic field depth L is not too large, where the acoustic wavelength is not too small (that is, the acoustic frequency

is not too high) and where the ultrasonic intensity is not too large. These conditions are usually satisfied. However, if this is not the case, then one would expect "vanishing of the refraction spectrum or Bragg incidence angles" instead of Bragg reflection. Of course, this has never been observed and we will deal with this question in a publication to appear soon.

§ 2. Apparatus and Measurement Method

The experimental arrangements are usually the same and were already described in the first communication, so that we will only add a few comments here. Two quartz disks are used, one of which has a thickness of 1 mm and /618
the other 3 mm. Both have the diameter 60 mm. Three experiments were carried out, one at the frequency 4.710 MHz and the other two at the frequency of 3.22 MHz. In the experiment with the ultrasonic frequency 4.710 MHz, the green light of a mercury lamp was used. In the experiments at the frequency 3.22 MHz, in addition to the green light we also used red lights. In the experiments with green light the halo-free "Neochrom, Fuji" photographic plates are used. In the experiments with red light the "panchromatic process plates, Fuji" are used.

In order to maintain the oblique incidence of the light on the acoustic wave front, the quartz disk suspended in the acoustic medium (transformer oil) was rotated by maintaining the liquid level constant. This means that the directly observed incidence angle is ϕ' for liquid and not the incidence angle ϕ for air. In order to carry out the comparison with the theory (Equation 6), it is necessary to find the index of refraction n_0 of the transformer oil. This was measured with the microscope, and the following values were obtained

$$n_0 \begin{cases} n_G = 1{\cdot}541 - 0{\cdot}0008\,(t - 11°{\cdot}3) \\ n_R = 1{\cdot}523 - 0{\cdot}0008\,(t - 11°{\cdot}6) \end{cases}$$

Here n_G and n_R, respectively, are the indices of refraction of the transformer oil for the green and the red light of the mercury lamp, respectively; t is the temperature in Celsius.

The quantitative measurement of the light intensity was only carried out in the experiment at 4.710 MHz. This method is a photographic-photometric one. Since this method was only mentioned briefly in the first communication, we will give several details here. In addition to several photographs of the diffraction spectra, each photographic plate also contained an intensity mark. It was produced by making a contact copy of an optical wedge using the same light source and the same exposure duration on the plate. This is done by deflecting the light beam by means of a mirror immediately after it emerges from the slit. It is then directed to the distant wedge. The wedge direction is parallel to the slit. There is a photographic plate directly behind the wedge. The common exposure duration must be selected in such a way that the diffraction spectra produce suitable blackening. Thus the intensity of the light source during production of the intensity mark must usually be reduced in order to make the corresponding blackening become suitable for use. This is done by adding several filters in front of the light source. Since the light is already monochromatic, it makes no difference which filter is used from this point of view. A step wedge of the I.P.C.R. (Tokyo) was used /619 as the optical wedge. This consists of a glass plate on which fine graphite grains have been deposited with a stepwise density. In this case, we use a wedge II B with the wedge depth difference 0.15 (i.e., transmission ratio of two adjacent wedge steps is 0.708).

Figure 1 shows an example of a measurement photograph. The three photographs of the diffraction spectra correspond to the three angular positions of the quartz. After that the diffraction spectra and the intensity mark were recorded with the microphotometer. In order to determine the light intensity from the microphotograms, it is necessary to calibrate the microphotometer because the deflection of the electrometer thread of the microphotometer is not proportional to the incoming amount of light in general. In order to obtain the light intensity-deflection characteristic line of the microphotometer, we again use an optical wedge. In this case, a wedge "II D" with a wedge-step difference 0.1 was recorded with the microphotometer instead of the photographic plate. By using the microphotograms of the wedge obtained in this way,

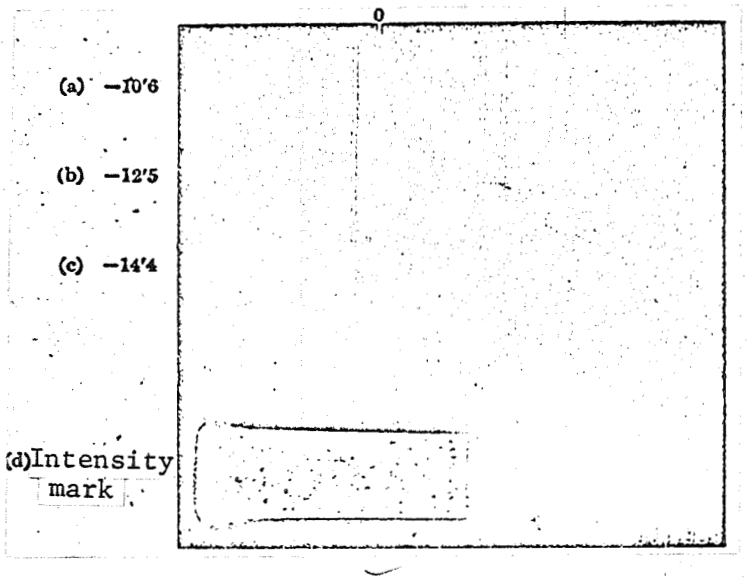

Figure 1. A measurement recording.
Picture reduction 0.66.

Figure 2, we obtained the relationship between the relative value of the amount of light i_r which is received by the photocell of the microphotometer after passing through the wedge, and the deflection of the microphotometer A using a method described in Table 1. Figure 3 shows the sensitivity curve of the microphotometer obtained in this way. This curve must remain the same for the same setting of the microphotometer. Nevertheless, as a precaution, it /620
was obtained fresh every day, and we always almost found the same one. During the recording of the microphotograms, we made provisions such that the dark line or the zero line of the deflection had the same magnitude for microphotograms of the wedge, microphotograms of the intensity marks, and microphotograms of the diffraction spectrum. Figure 4 shows an example of the microphotometer curve for the intensity mark. The blackening curve for the photographic plate (Neochrom, Fuji) was obtained from it. The computational scheme /621
used is shown in Table 2. Here, I_r is the relative amount of light for the

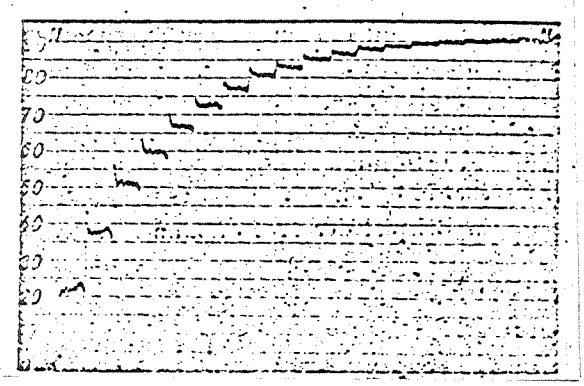

Figure 2. Microphotogram of an optical wedge (II D). Picture reduction 0.5.

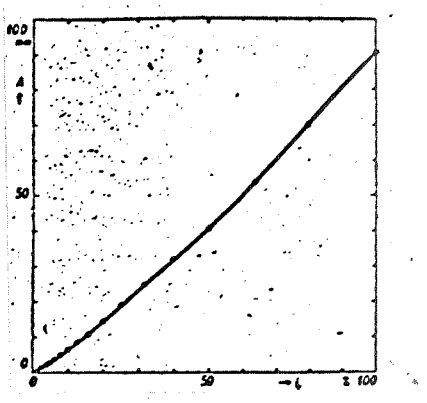

Figure 3. Sensitivity curve of a microphotometer. A - deflection, i_r - relative recorded light intensity.

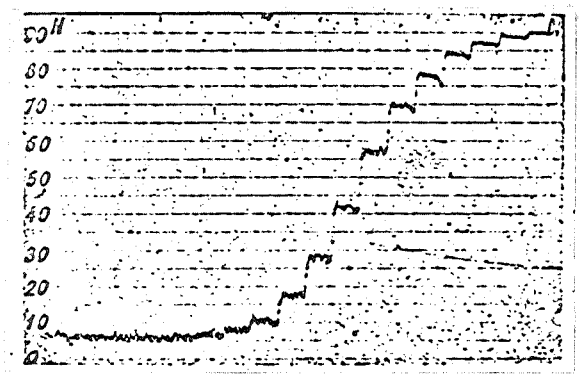

Figure 4. Microphotometer curve of an intensity mark. Picture reduction 0.5.

original photograph and

$$S=1-\frac{i_r}{i_{max}}$$

is the blackening of the plate, in which i_{max} is the recorded amount of light for maximum deflection of the microphotometer curve, i.e., for the entire unexposed region of the photographic plate.

The selection of the normalization quantity I_r is arbitrary. However, in order to obtain the light intensity exactly, it is appropriate to select the blackening for I_r = 100% slightly

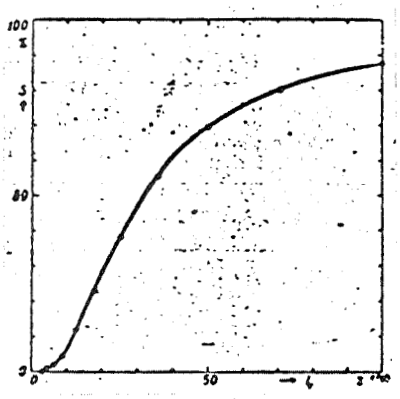

Figure 5. Blackening curve of a photographic plate. S - blackening; I_r - relative light intensity.

more than the maximum blackening of the diffraction spectra taken on the same photographic plate. The exposure /622 time for photographs of the diffraction spectra must, of course, be selected in such a way that the strongest line will be as far away as possible from the saturated portion of the blackening curve and so that, at the same time, the blackest order of diffraction present which can be observed visually will still result in a measurable blackening. Figure 6 shows an

TABLE 1. METHOD OF OBTAINING THE SENSITIVITY CHARACTERISTIC LINE OF THE MICROPHOTOMETER FROM MICROPHOTOGRAMS OF THE OPTICAL WEDGE

	Ordinate of the microphotometer curve	Deflection A	Relative recorded light intensity i_r
Zero line	91·6mm	0 mm	0%
Wedge step 0·1	1·0	90·6	100
0·2	21·7	69·9	79·4
0·3	38·5	52·1	63·1
0·4	51·0	40·6	50·1
0·5	59·4	32·2	39·8
0·6	66·7	24·9	31·6
0·7	72·5	19·1	25·1
0·8	77·1	14·5	20·0
0·9	80·8	10·8	15·8
1·0	83·1	8·5	12·6
1·1	85·0	6·6	10·0
1·2	86·6	5·0	7·9
1·3	87·7	3·9	6·3
1·4	88·6	3·0	5·0
1·5	89·3	2·3	4·0
1·6	89·7	1·9	3·2
1·7	90·1	1·5	2·5
1·8	90·4	1·2	2·0
1·9	90·7	0·9	1·6
2·0	91·1	0·5	1·3

TABLE 2. METHOD OF OBTAINING THE BLACKENING CURVE OF THE PHOTOGRAPHIC PLATE

	Ordinate of the microphotometer curve	Deflection A	Relative recorded amount of light i_r	$\frac{i_r}{i_{max}}$	Blackening S	Relative light intensity I_r
Zero line Wedge, Plane	91·6 mm 0·2	85·4 mm	94·6	100 %	0 %	3·2 %
Wedge depth (5)	7·1	84·5	93·6	99·0	1·0	4·5
	8·1	83·5	92·7	98·0	2·0	6·3
	10·5	81·1	90·4	95·6	4·4	8·9
	17·6	74·0	83·4	88·1	11·9	12·6
	28·3	63·3	72·8	77·0	23·0	17·8
(10)	42·4	49·2	58·5	61·9	38·1	25·1
	57·3	34·3	42·2	44·6	55·4	35·5
	69·5	22·1	28·8	30·5	69·5	50·1
	78·3	13·3	18·7	19·8	80·2	70·8
	84·0	7·6	11·6	12·3	87·7	100·0

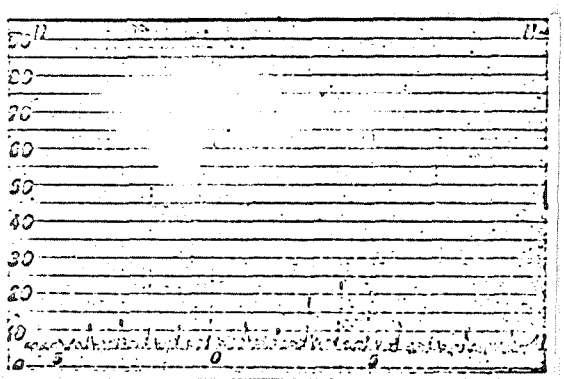

Figure 6. A microphotometer curve of the diffraction spectra. (4.710 MHz, incidence angle $\phi' = -12.5$).

Picture reduction 0.5.

example of the microphotometer curve of the diffraction spectra. This corresponds to photograph (b) of Figure 1. From this curve and using the sensitivity characteristic line of the microphotometer (Figure 3) and the photographic blackening curve (Figure 5), we obtain the intensity distribution of the diffraction spectra as a function of order. The computational scheme is given in Table 3. /623

The quantity I_n in the last column of the Table is defined by $I_n = \frac{I_r}{\sum I_r}$ and is the light intensity normalized for uniform incident light.

TABLE 3. METHOD OF OBTAINING INTENSITY REDUCTION AS A FUNCTION OF ORDERS OF THE DIFFRACTION SPECTRA ($\phi' = -12.'5$)

		Ordinate of the micro-photometer curve	Deflec-tion A	Relative recorded amount of light i_r	$\frac{i_r}{i_{max}}$	Blackening S	Relative light intensity I_r	Normal-ized light intensity I_n
Zero line background		91·6 mm 5·7	85·9 mm	95·2 %	100 %	0 %	%	%
Right	8	9·5	82·1	91·3	95·9	4·1	8·6	2·3
	7	55·2	36·4	44·7	47·0	53·0	33·7	9·1
	6	76·9	14·1	20·5	21·5	78·5	67·5	18·2
	5	65·1	26·6	33·6	35·3	64·7	44·0	11·9
	4	23·5	68·1	77·7	81·6	18·4	15·6	4·2
	3	19·0	72·6	82·0	86·1	13·9	12·5	3·6
	2	10·0	81·6	90·9	95·5	4·5	8·9	2·4
	1	12·0	79·6	89·0	93·5	6·5	10·4	2·7
Center	0	61·7	29·9	37·3	39·2	60·8	40·2	10·8
Left	1	78·9	12·7	18·1	19·0	81 0	73·1	19·7
	2	50·4	41·2	50.2	52·7	47·3	30·0	8·1
	3	12·8	78·8	88·1	92·5	7·5	10·8	2·9
	4	11·4	80·2	89·6	94·1	5·9	9·9	2·7
	5	6·6	85·0	94·3	99·1	0·9	4.5	1·2
							Σ=390·7	99·8

3. Experimental Results

(1) Experiments at the ultrasonic frequency 3.22 MHz.

The experiments carried out at this ultrasonic frequency were only for orientation purposes in the sense that they did not require intensity measurements of the diffraction spectra. Two experiments were carried out in this case, one with green light and the other with red light. Figure 7 shows the diffraction spectra obtained with green light for the wavelength 5461 Å. The numbers on the side refer to the incidence angles of the light with respect to the propagation direction of the ultrasonic wave. Figure 7 shows the characteristic change of these spectra as a function of the incidence angle.

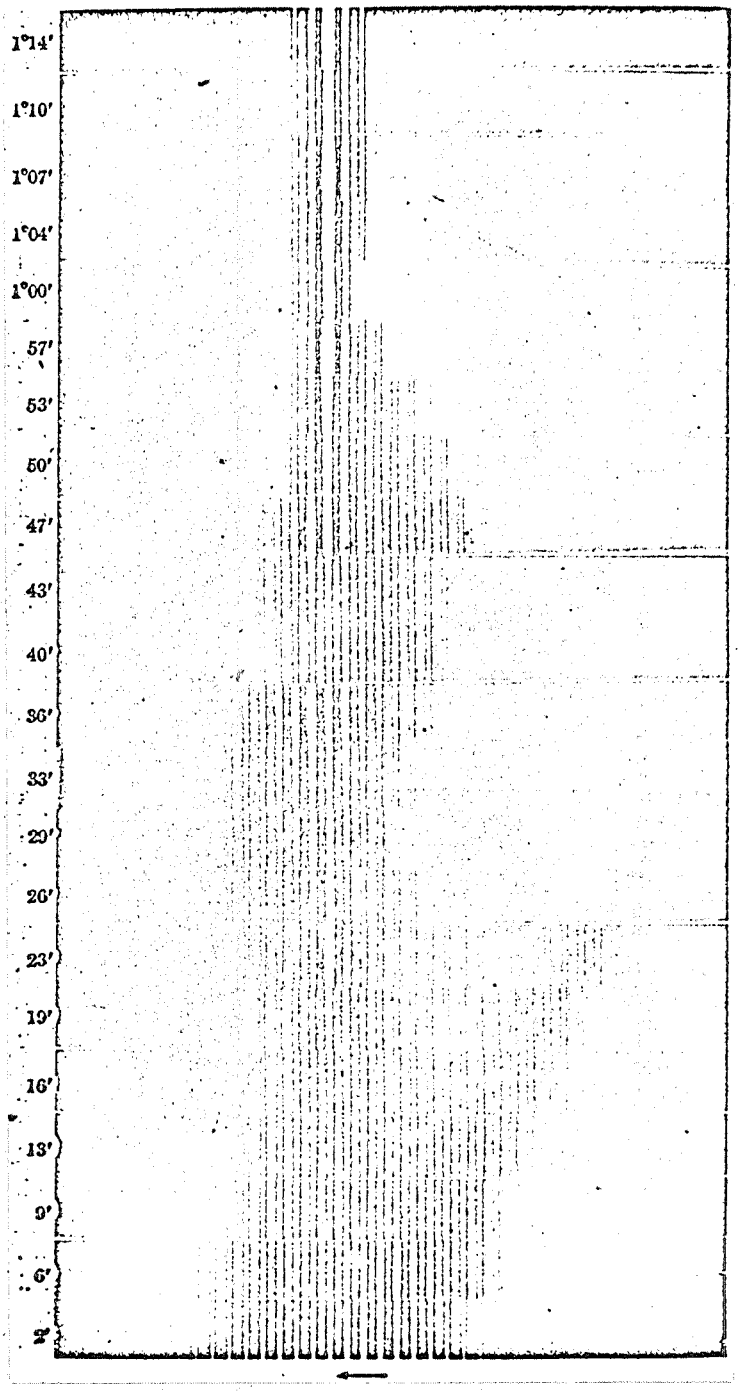

Figure 7. Diffraction spectra at 3.22 MHz (light wavelength 5461 Å) ← direction of sound propagation. Picture reduction 0.7.

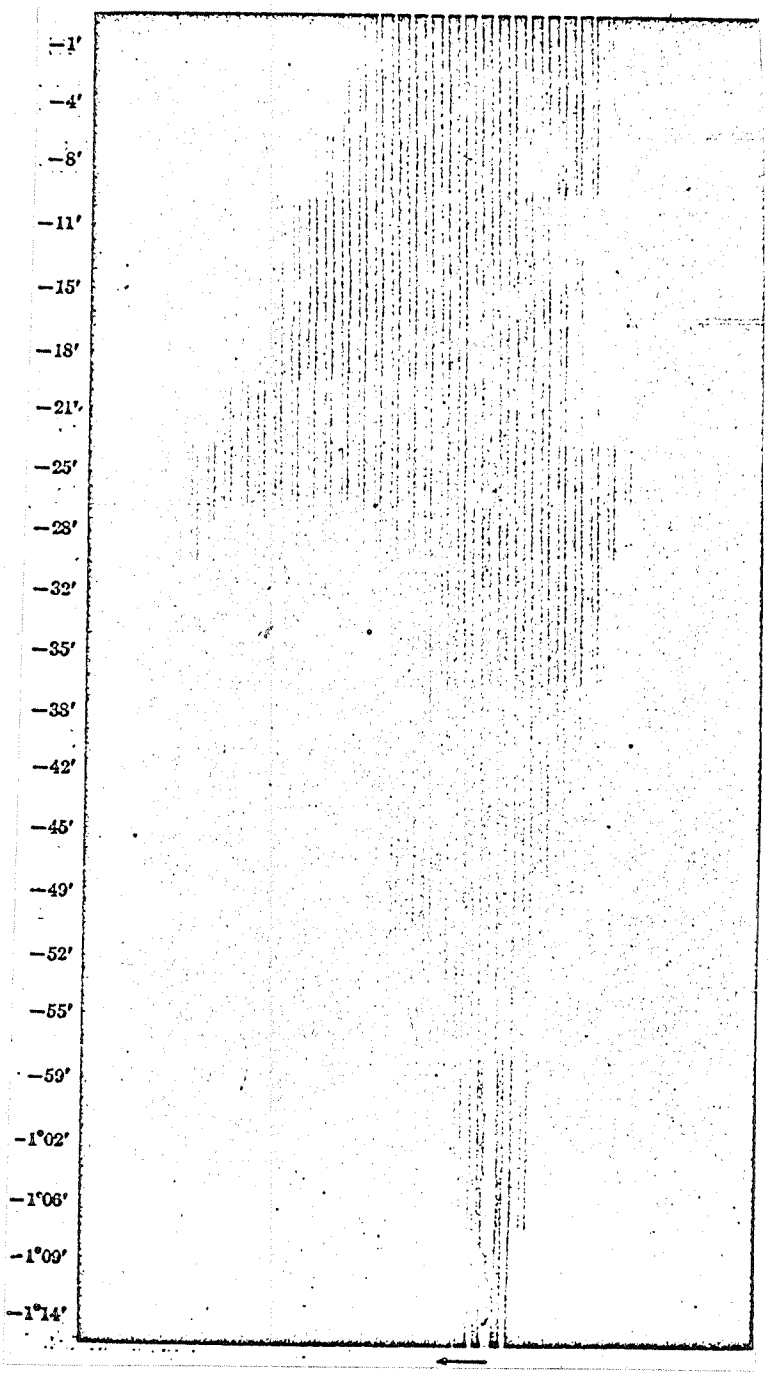

Figure 7(2).

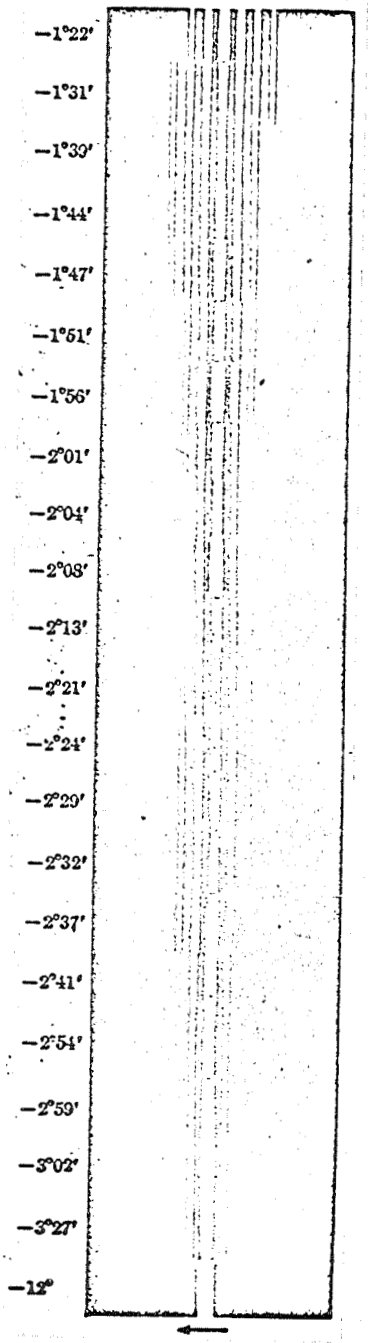

Figure 7(3).

The essential point of the asymmetry of the diffraction spectra obtained with oblique incidence is manifested in the Bragg reflection, which extends to the 21st diffraction order in this case. The long branches on the photographs correspond to the Bragg reflection. The following discussion will show that this selective reflection is indeed the Bragg reflection. In Figure 8 the selected strong diffraction orders are shown as a function of the incidence angle. The linear /626 dependence between the two quantities can immediately be seen. The Bragg angle for order -1 is obtained from

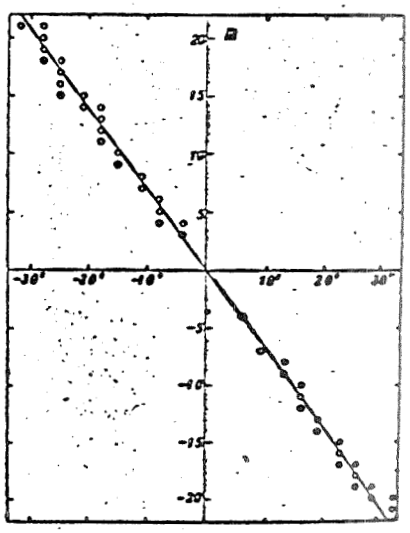

Figure 8. The selected strong orders of diffraction as a function of the incidence angle

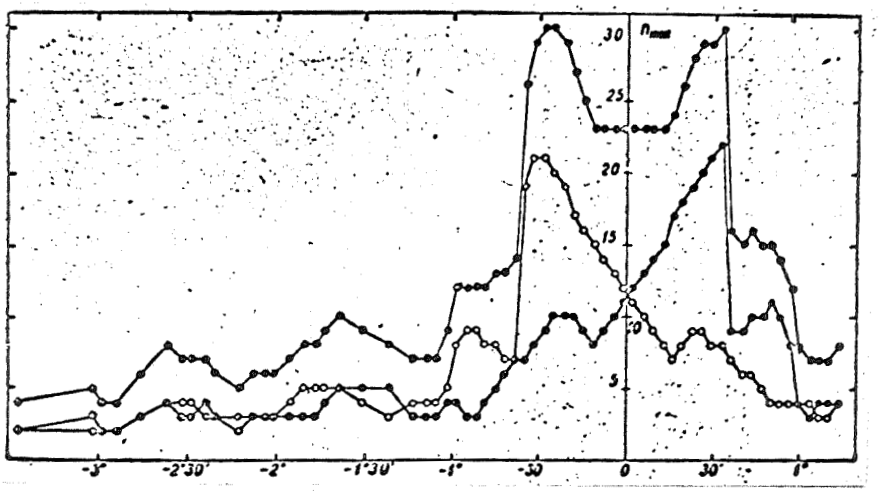

Figure 9. Number of diffraction spectra as a function of the incidence angle.

the inclination of the line shown:

$$(\varphi'_B)_{\text{obs.}} = -\frac{(\varphi'_B)_n}{n} = 1'\cdot 475. \ (28°C)$$

This is the observed Bragg angle in the transformer oil. On the other hand, the calculated value of the Bragg angle in air is obtained from the values of the light wavelength λ = 5461 Å and the acoustic wavelength Λ = 0.4193 mm, which in turn is calculated from the interval of the bending spectra on the photographic plate and the distance of it from the objective, in the following ways

$$\varphi_B = \frac{1}{2}\frac{\lambda}{\Lambda} = 0\cdot 000653.$$

In order to calculate the Bragg angle in the liquid itself, it is still necessary to know the index of refraction of the medium. This, however, has been /627

measured in a previous experiment (§ 2) and is found to be

$$n_0=(n_G)_{23^\circ}=1{\cdot}53,$$

so that the calculated Bragg angle in transformer oil is given by

$$(\varphi'_B)_{ber.}=\frac{1}{2}\frac{\lambda}{n_0\Lambda}=1{\cdot}'467\ (28^\circ C).$$

This agrees quite well with the observed values.

Now let us turn to the number of refraction spectra . Figure 9 shows these numbers for the right and left refraction orders as well as for the total refraction orders (except for order of 0). As the figure shows, the total number of refraction spectra does not have a maximum for normal incidence, but instead at somewhat oblique incidence angles which lie both sides of normal incidence. This agrees with earlier results of an experiment carried out with standing ultrasonic waves [5].

In the experiment with red light (6152 Å, 6232 Å), we obtain the diffraction spectra shown in Figure 10. The broadening of the lines of higher order is due to the fact that the filtered red light from the mercury lamp is not completely monochromatic. Here again we can see well-developed Bragg reflection. Figure 11 shows the linear relationship between the order number of the selected strong diffraction spectra and their incidence angles. In the following we will give the measurement results in this case as well as the calculated numbers: /629

$\Lambda=0{\cdot}4139$ mm (28°C), $\lambda=6200$ Å (6152 und 6232 Å),

$n_0=(n_B)_{23^\circ}=1{\cdot}51$;

$(\varphi'_B)_{obs.}=\quad 1{\cdot}'735,$

$(\varphi'_B)_{calc.}=\frac{1}{2}\frac{\lambda}{n_0\Lambda}=1{\cdot}'683.$

The agreement is satisfactory.

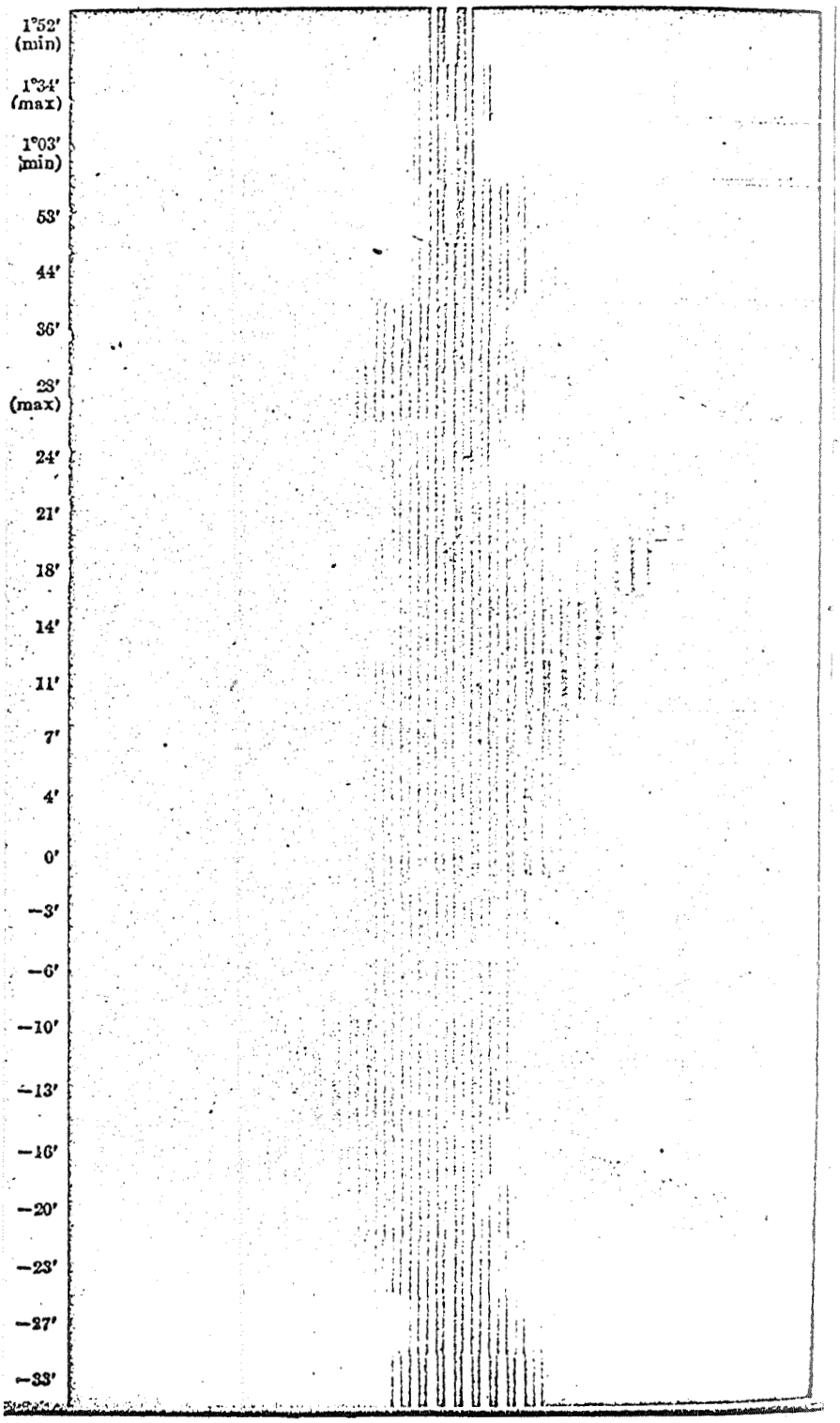
1°52'
(min)
1°34'
(max)
1°03'
(min)
53'
44'
36'
28'
(max)
24'
21'
18'
14'
11'
7'
4'
0'
−3'
−6'
−10'
−13'
−16'
−20'
−23'
−27'
−33'

Figure 10(1).

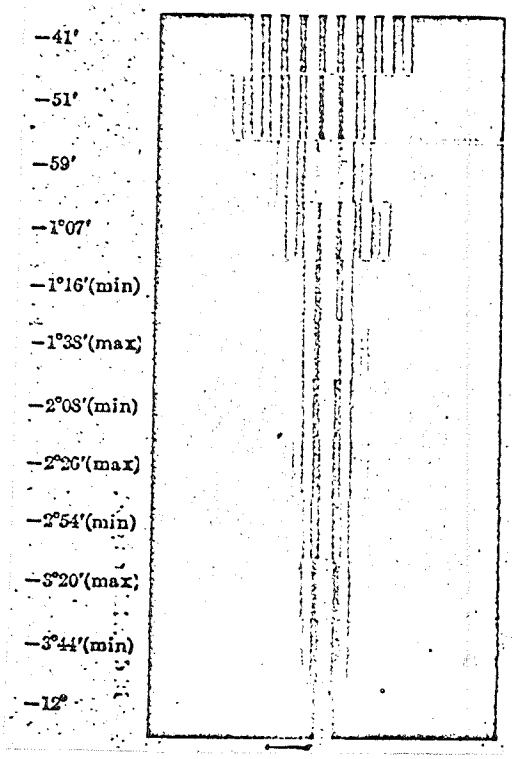

Figure 10(2).

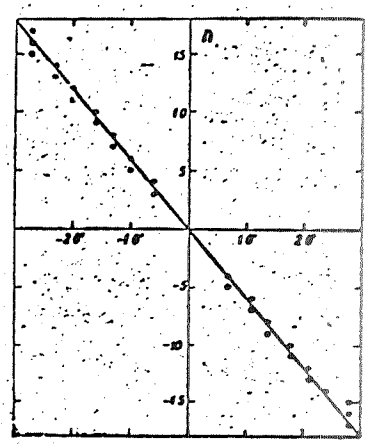

Figure 11. The selected strong orders of diffraction as a function of the incidence angle.

(2) Experiment at the ultrasonic frequency 4.71 MHz.

In this case, only green light was used. Figure 12 shows the diffraction spectra obtained with this ultrasonic frequency. Here again, the Bragg reflection is so noticeable that one will not hesitate to state that it is the most important characteristic of the intensity distribution of the diffraction spectra for oblique wave incidence. The individual diffraction spectra were measured according to the methods given above, and the intensity distributions were calculated as a function of the orders. The measurement results are shown in Table 4 and Figure 13. In addition, Figure 14 shows the dependence /635

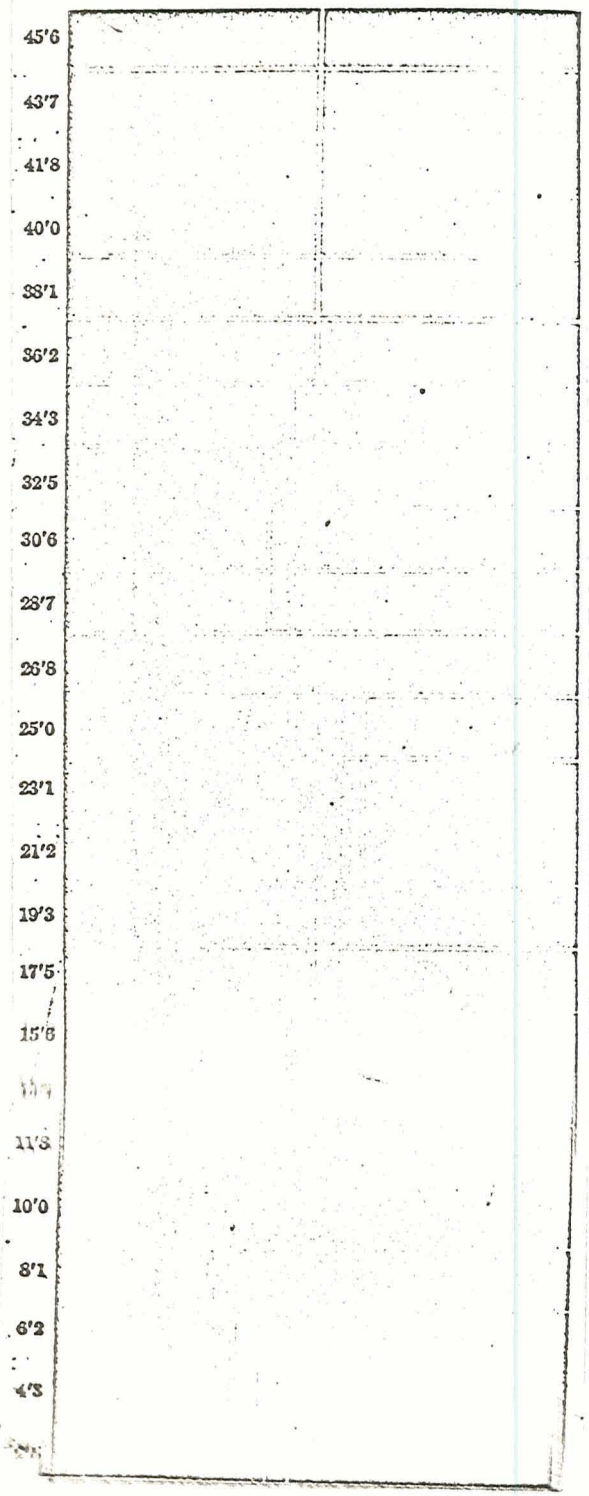

of the intensity of individual diffraction orders as a function of the incidence angle. Figure 15 shows this for the total diffracted light as well as for the light of the total right (I_r) and left (I_r) diffraction orders, respectively. The Bragg angle of individual diffraction orders was determined from Figure 14 and is shown as a function of the diffraction order in Figure 16. The straight line relationship between the two quantities can be immediately seen from the figure. In Figures 12 and 14 we see several side maxima in addition to the Bragg principal maximum to both sides of it. They are symmetrical with respect to it. The positions of these side maxima are empirically given by the formula

$$\varphi'_n = \varphi'_B \pm \frac{3}{2}\frac{\Lambda}{L}$$

except for the zero order and the two first orders, where additional strong

Figure 12. Diffraction spectra at 4.71 MHz. (Light wavelength 5461 Å) → direction of sound propagation. Picture reduction 0.6.

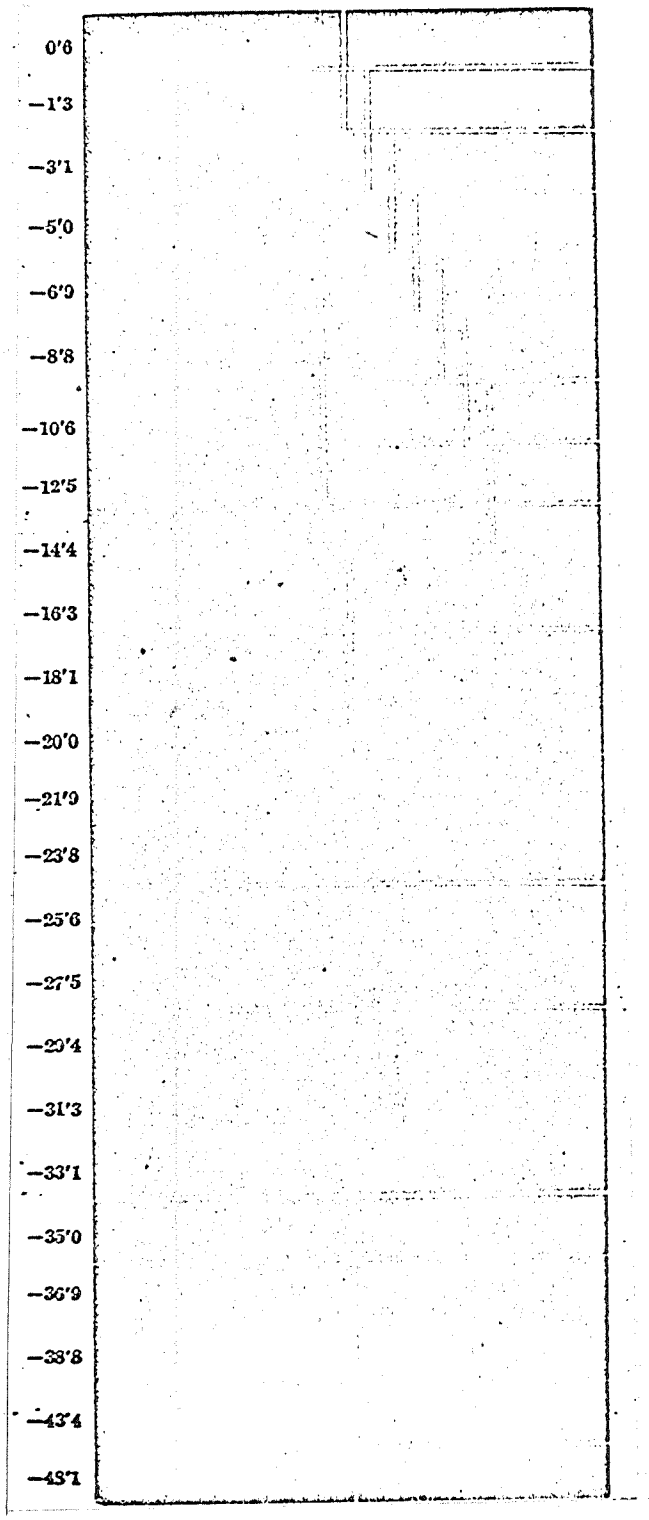
0'6
-1'3
-3'1
-5'0
-6'9
-8'8
-10'6
-12'5
-14'4
-16'3
-18'1
-20'0
-21'9
-23'8
-25'6
-27'5
-29'4
-31'3
-33'1
-35'0
-36'9
-38'8
-43'4
-48'1

Figure 12(2).

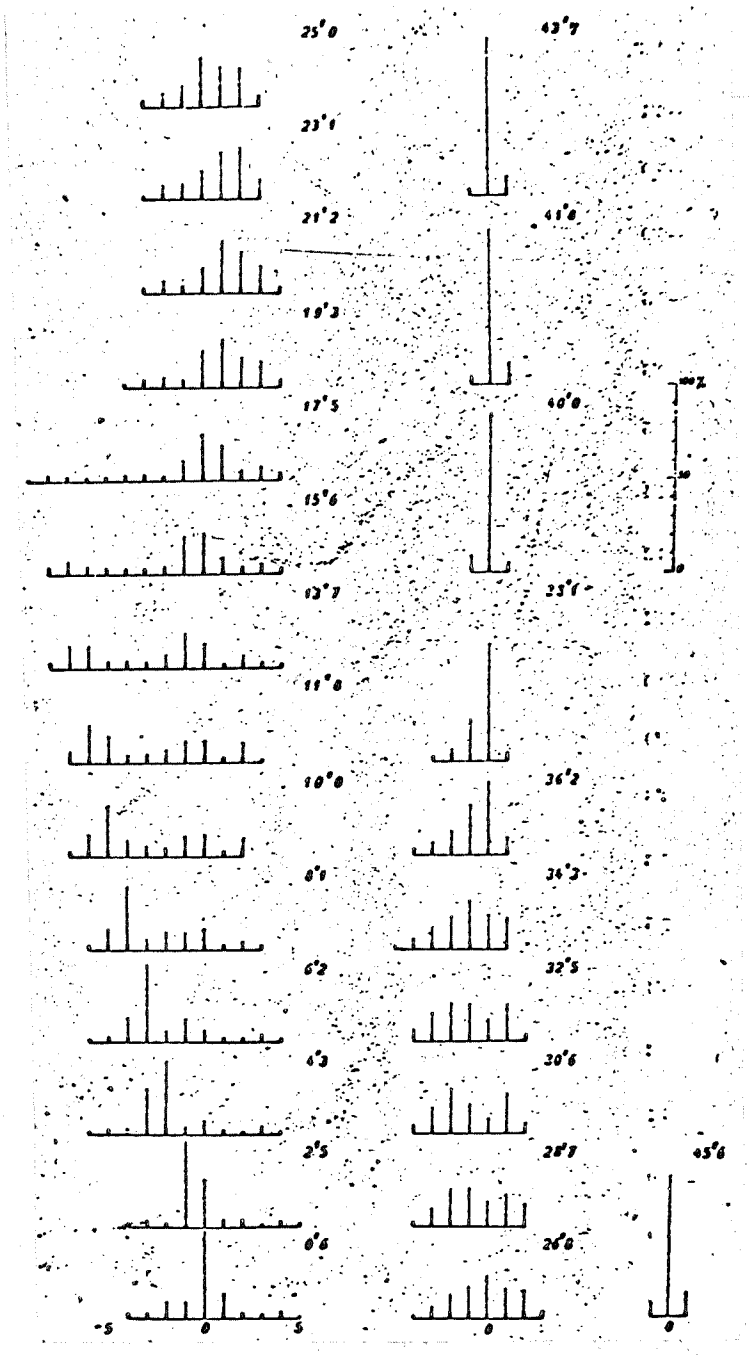

Figure 13. Intensity distributions as a function of the orders of the diffraction spectra for various incidence angles.

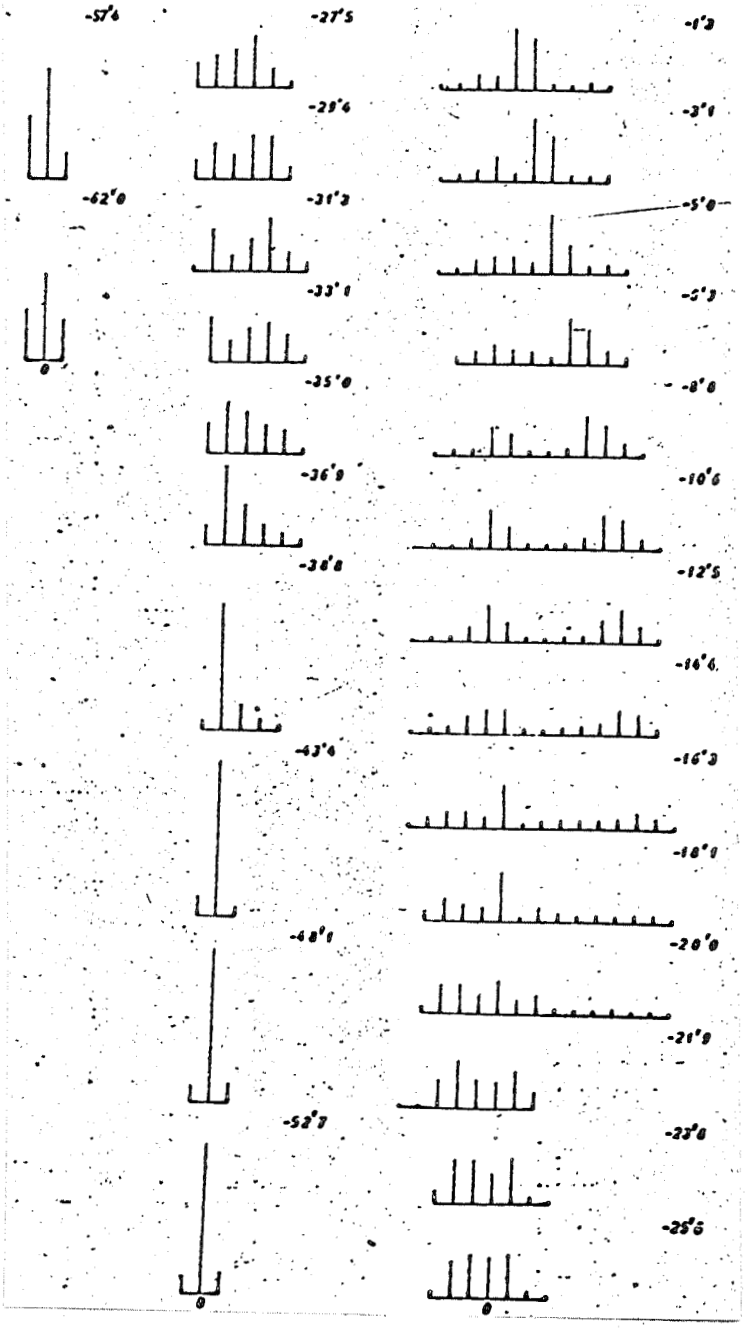
-57'6
-27'5
-1'2
-29'6
-3'1
-62'0
-31'2
-5'0
-33'1
-5'3
0
-35'0
-8'8
-36'9
-10'6
-38'8
-12'5
-16'6
-43'6
-16'3
-18'1
-46'1
-20'0
-21'9
-52'7
-23'8
-25'6
0
0

Figure 13(2).

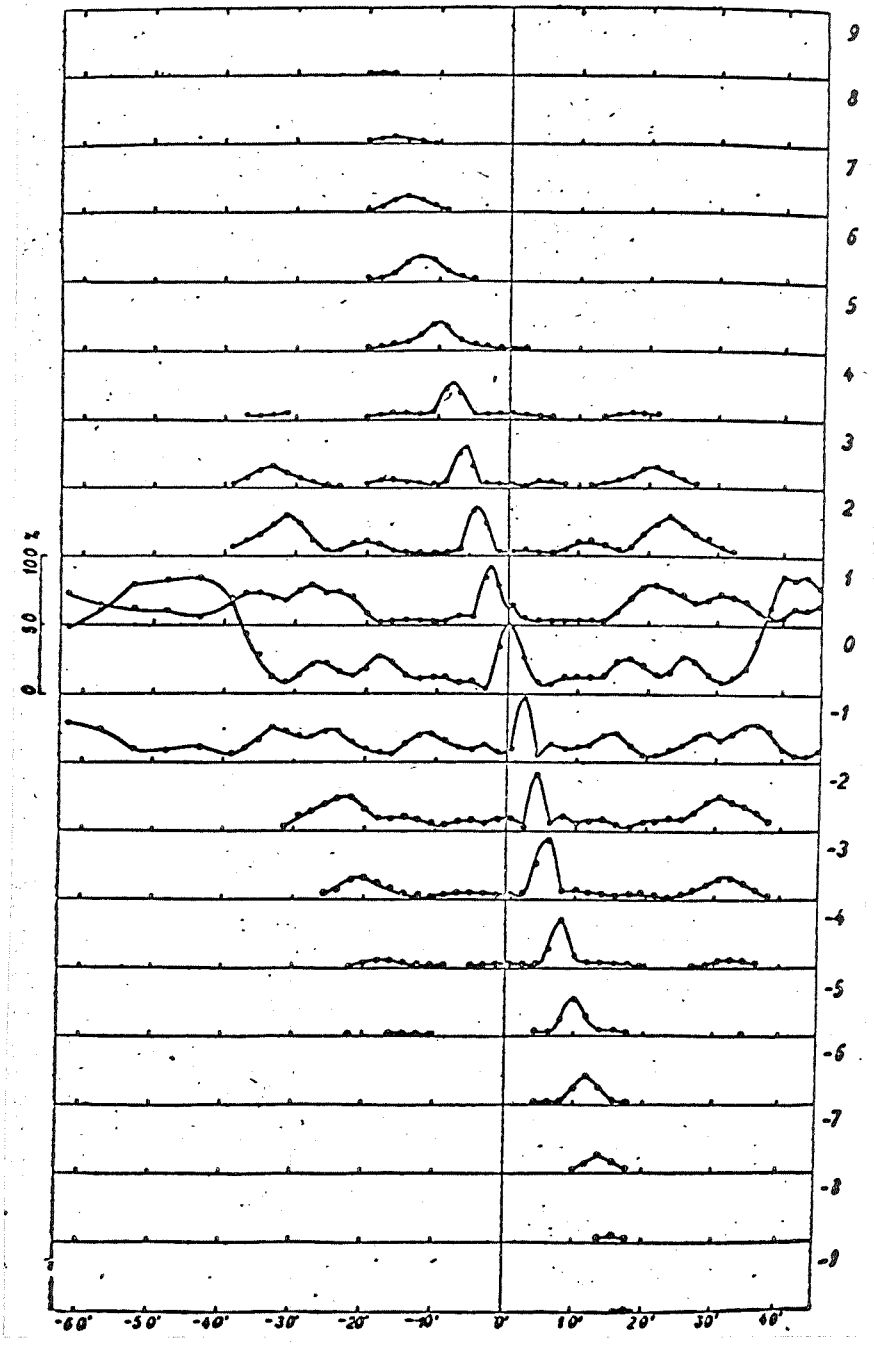

Figure 14. Intensity of individual diffraction spectra as a function of incidence angle.

TABLE 4. INTENSITY DISTRIBUTION AS A FUNCTION OF ORDER OF THE DIFFRACTION SPECTRA AS A FUNCTION OF THE INCIDENCE ANGLES

Order No. / Incidence angle	−9	−8	−7	−6	−5	−4	−3	−2	−1
45·6									8·5
43·7									4·7
41·8									4·9
40·0									9·4
38·1							2·8	6·7	22·9
36·2						4·2	6·9	13·1	27·4
34·3					2·1	5·9	12·1	17·9	26·2
32·5						6·5	16·0	20·9	20·6
30·0						5·5	14·9	25·6	16·7
28·7						2·8	10·4	21·1	21·2
26·8						1·9	7·2	13·4	17·8
25·0							4·4	8·4	11·8
23·1							1·9	9·0	8·9
21·2							3·5	7·4	4·7
19·3						2·3	4·9	6·3	4·6
17·5	1·2	3·6	2·9	2·1	2·7	3·6	4·3	3·3	11·8
15·6		4·7	7·8	4·1	4·1	3·7	3·4	4·7	20·9
13·7		3·6	12·9	12·6	4·1	4·5	4·0	8·2	19·5
11·8			6·7	20·7	14·6	4·3	4·9	7·4	12·3
10·0			2·4	12·2	27·3	8·9	6·3	5·8	11·3
8·1				3·3	12·0	31·9	6·4	10·3	10·0
6·2				2·0	3·4	14·1	42·7	6·2	12·9
4·3				1·7	3·5	3·3	25·7	40·2	4·8
2·5						2·4	4·3	2·4	46·4
0·6						3·0	3·4	9·5	9·5
− 1·3						3·0	3·5	8·6	8·1
− 3·1						2·4	4·1	5·8	12·3
− 5·0						1·5	2·5	7·7	9·6
− 6·9							4·5	7·2	10·9
− 8·8						1·4	3·5	4·2	16·2
−10·6					0·9	2·0	1·3	5·6	21·2
−12·5					1·2	2·7	2·9	8·1	19·7
−14·4					1·8	3·6	4·5	10·1	13·9
−16·3					2·0	5·5	8·4	9·0	6·3
−18·1						5·6	12·1	9·6	7·4
−20·0					1·0	3·8	15·5	15·8	9·9
−21·9						1·2	14·6	25·2	15·1
−23·8							7·1	23·6	23·6
−25·6							4·4	20·1	23·3
−27·5								14·5	18·9
−29·4								11·2	19·7
−31·3								3·4	22·4
−33·1									25·1
−35·0									16·6
−36·9									11·0
−38·8									5·9
−42·4									10·9
−48·1									8·4
−52·7									9·9
−57·4									24·8
−62·0									28·7

(Table continued on next page)

TABLE 4. INTENSITY DISTRIBUTION AS A FUNCTION OF ORDER OF THE DIFFRACTION SPECTRA AS A FUNCTION OF THE INCIDENCE ANGLES

(continued)

0	1	2	3	4	5	6	7	8	9
77·4	14·1								
84·4	10·9								
83·1	12·0								
85·1	5·5								
62·5	5·1								
38·9	9·6								
18·7	17·1								
11·9	20·4	3·7							
8·8	22·6	5·9							
14·1	17·9	12·5							
23·9	16·2	15·9	3·7						
26·5	21·6	21·1	6·3						
15·7	25·2	28·2	11·2						
14·3	28·5	22·6	15·0	3·9					
20·2	26·8	16·2	14·0	4·8					
25·4	19·3	6·4	8·5	4·7					
22·8	9·5	4·2	6·1	4·1					
13·7	2·7	7·8	3·8	2·5					
12·0	3·0	11·3	2·7						
12·3	3·2	10·0							
12·1	2·9	5·4	2·8						
7·0	2·8	2·5	4·5	1·9					
8·3	3·2	2·2	5·0	2·1					
20·6	4·9	5·0	1·9	3·7	2·4				
48·2	13·8	3·5	2·7	4·3	2·1				
34·0	28·8	3·5	3·1	4·7	2·7				
4·4	34·2	24·4	3·6	4·2	4·2				
9·8	6·4	32·6	16·3	4·8	5·5	2·3			
8·2	7·2	4·4	25·4	19·7	8·0	4·5			
12·6	3·1	3·0	5·2	22·5	17·5	8·1	2·6		
12·1	2·9	2·4	3·5	6·0	19·0	16·3	5·7	1·1	
10·8	2·7	2·4	3·6	4·2	11·9	18·2	9·1	2·3	
13·9	3·5	2·6	3·9	5·1	6·8	14·3	12·1	3·7	
23·3	2·8	4·3	5·4	5·2	5·4	5·9	9·2	5·9	1·6
20·8	2·3	8·3	5·6	4·1	3·9	3·7	4·2	4·5	2·0
18·2	8·3	10·8	3·1	2·3	2·5	3·8	2·0	2·3	1·7
13·9	20·2	8·9							
16·2	24·4	4·1	1·1						
21·8	23·7	4·4	2·2						
21·9	29·0	11·6	4·1						
13·9	24·5	23·7	7·1						
9·2	18·0	29·4	11·1	5·5					
12·5	19·6	22·7	15·9	4·2					
28·4	23·0	15·4	13·3	3·1					
43·7	22·7	11·7	7·3	3·8					
69·0	14·7	6·8	3·6						
83·7	5·4								
81·8	9·8								
78·5	11·5								
60·8	14·4								
48·3	23·0								

Figure 15. The total intensity of the diffracted light as well as intensities of the right and left orders of diffraction as a function of incidence angle.

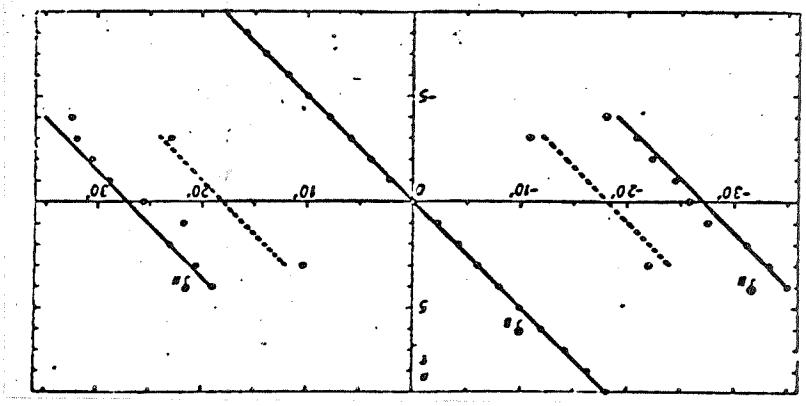

Figure 16. The Bragg angle, incidence angles of the side maxima and those of the minima as a function of the order number.

side maxima occur. Here ϕ_S' is the Bragg incidence angle in liquid, ϕ_N' the incidence angle for side maxima of the light intensity, Λ the acoustic wavelength and L the acoustic field depth. Figure 16 shows, in addition to the Bragg maximum, the two side maxima. In this case, the results obtained are as follows: /638

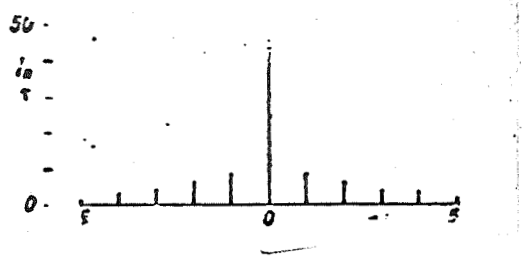

Figure 17. Intensity distribution of the diffraction spectra for normal incidence of the light on the sound direction.

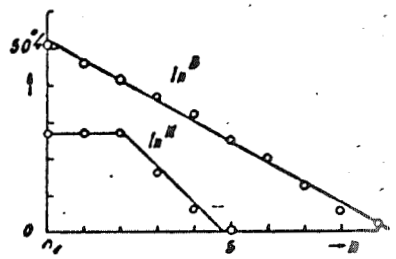

Figure 18. Intensities of the Bragg maxima and side maxima as a function of the order number.

$$\Lambda = 0{\cdot}3153\ \text{mm},\ \lambda = 5461\ \text{Å},\ n_0 = (n_o)_{H_2O} = 1{\cdot}54;$$

$$(\varphi'_B)_{\text{observed}} = 2{\cdot}'00\ (12°\text{C}),$$

$$(\varphi'_B)_{\text{calculated}} = \frac{1}{2}\frac{\lambda}{n_0 \Lambda} = 1{\cdot}'95\ (12°\text{C}).$$

Agreement between the found and calculated values is satisfactory.

From Figure 15 it can be seen that the total diffracted light intensity has a minimum for normal light incidence. This is also true for the total number of diffraction spectra, which again agrees with our earlier results.

TABLE 5. INTENSITY DISTRIBUTION OF THE DIFFRACTION SPECTRA FOR NORMAL INCIDENCE

Diffraction order n	Intensity I_n (%)		
	Right	Left	Center
0			51
1	11	7	9
2	8	10	6.5
3	4	3.5	3.8
4	4.5	3	3.8
5	2	1	1.5

In Figure 14 we also obtain the intensity distribution of the diffraction spectra as a function of order for normal incidence. Since it should be theoretically symmetrical, we calculated the average from both diffraction orders with the same order number (Table 5) and the ideal intensity distribution obtained in this way is shown in Figure 17.

Finally we show the intensities of the Bragg maxima and the side maxima in Table 6, and we show the average in Figure 18. /639

TABLE 6. INTENSITY OF THE BRAGG MAXIMA AND SIDE MAXIMA OF EACH DIFFRACTION SPECTRUM

Order number n	Bragg Maximum I_n^B (%)			Side maxima I_n^N (%)					I_n^N/I_n^B
	+	−	Average	+		−		Average	
0			51	27		27		27	0·53
				Right	Left	Right	Left		
1	44	38	46	28	29	27	24	27	0·59
2	42	41	41·5	28	29	25	27	27	0·65
3	30	44	37	16	16	16	16	16	0·43
4	27	37	32	6	5	6	5	5·5	0·17
5	22	28	25				2	0·5	0·02
6	19	21	20						
7	12	13	12·5						
8	6	5	5·5						
9	2	2	2						

The intensity of the side maxima is much stronger than those which could be expected from an extrapolation of the David theory. Equation (4) (§ 1) of the David theory would lead to a value $I_1^N/I_1^B = 0.0412$ which is thirteen times smaller than what is observed. Of course, a quantitative comparison of the experiments with the theories developed up to the present is unfair, because these theories only restrict themselves to the case where the weak first and second refraction orders occur.

Kobayasi Institute of Physical Research
Kokubunzi near Tokyo

Received May 25, 1942

REFERENCES

1. Nomoto, Otohiko. Proc. Phys.-Math Soc. Japan, Vol. 24, 1942, p. 380.
2. Debye, P. and F.W. Sears. Proc. Nat. Acad. Sci., Vol. 18, 1932, p. 409.
3. Bär, R. Helv. Phys. Acta., Vol. 9, 1936, p. 265.
4. Parthasarathy, S. Proc. Indian Acad. Sci., Vol. (A) 3, 1937, p. 442.
5. Nomoto, Otohiko. Proc. Phys.-Math. Soc. Japan., Vol. 19, 1937, p. 264.
6. Neumann, E.A. Proc. Phys. Soc., Vol. 51, 1939, p. 794.
7. Becker, H.E.R. Ann. Phys., Vol. 25, 1936, p. 373.
8. Rytow, S.M. Phys. Zeits. Sowjet, Vol. 8, 1935, p. 626.
9. David, E. Phys. Zeits, Vol. 38, 1937, p. 587.
10. Extermann, R.C. Helv. Phys. Acta., Vol. 10, 1937, p. 185.
11. Parthasarathy, S. Proc. Indian Acad. Sci., Vol. (A) 3, 1936, p. 594.
12. Korff, W. Phys. Zeits., Vol. 37, 1936, p. 708.

Translated for National Aeronautics and Space Administration under Contract No. NASw 2035, by SCITRAN, P.O. Box 5456, Santa Barbara, California, 93108